Photocatalytic Degradation of Rhodamine B Dye in Wastewater Using Gelatin/CuS/PVA Nanocomposites under Solar Light Irradiation

Abdullah A. Al-Kahtani

Chemistry Department, College of Science, King Saud University, Riyadh, KSA

Email: akahtani@KSU.EDU.SA

Abstract

The crosslinked gelatin/CuS/PVA nanocomposite catalyst prepared using gamma irradiation as initiator was extensively characterized using several techniques including transmission electron microscopy (TEM), UV-Vis spectroscopy, infrared spectroscopy (IR) and X-ray diffraction (XRD). We chose Rhodamine B (RhB) dye as a model contaminant in order to investigate its Photocatalytic activity under solar light irradiation. The effects of pH, catalyst concentration and RhB concentration on degradation reaction were also investigated. Similar to the observed trend for the photocatalytic oxidation of other organic compounds, the efficiency of photocatalytic degradation of RhB tended to decrease with increasing the concentration of RhB. The degradation efficiency of RhB is found to increase as pH is increased up to pH of 10, then starts decreasing at pH values higher than 10. The degradation efficient of RhB is found to increase as the amount of the catalyst dosage increases up to an optimum value of 0.25 g. Increasing the concentrations of photocatalyst beyond 0.25 g was found to decrease the photocatalytic activity of RhB. It was proven that the degradation process of RhB reaction rate obeyed a pseudo-first-order reaction of the catalyst concentration of gelatin/CuS/PVA nanocomposite. The degradation kinetics was found to fit well Langmuir-Hinshelwood rate law. The results obtained showed that after using the catalyst five times repeatedly, the catalyst retained its efficiency and the rate of the degradation process was still above 80%.

Keywords

Rhodamine B, Degradation, Photocatalysis, CuS Nanocomposite, Gamma Ray
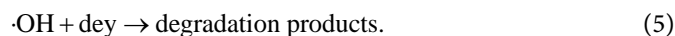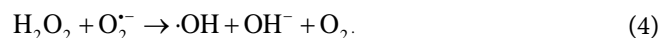
1. Introduction

Organic dyes used in food and textile manufacturing are considered to be an essential source of pollutants to the environment due to their non biodegradability and high

toxicity to aquatic creatures and carcinogenic effects on humans. Therefore, organic dyes removal from waste waters has been one of the most important environmental issues and complete removal of organic dyes is essential because organic dyes will be perceptible even at low quantities [1]. In countries all over the world, developing and industrialized, the number of organic pollutants discharged into all kinks of open waters is on the rise [2]. Soluble organic dyes, which are considered to be one of the main groups of pollutants in waste water, are among those organic pollutants.

A series of solutions have been put forward to protect humanity from organic dye polluted waste water, and photodegradation represents an important degradation pathway. The photocatalytic oxidation is considered to be one of the emerging technologies used to remove organic pollutants. These technologies have high efficiency in their mineralization, ideally producing CO_2, H_2O and inorganic mineral ions as end products [3] [4] [5] [6]. Photocatalytic degradation, in particular, has attracted a great deal of attention for its simplicity, efficiency, law cost and low secondary pollution. Photo-catalysis in general has attracted the attention of many researchers for many years due to its widespread applications in water purification and molecular hydrogen (H_2) generation [6]. Recently, semiconductor photocatalysts show a promising potential to utilize solar energy to deal with many related problems, like the degradation of organic pollutants and the generation of H_2 from water analysis [7] [8].

Rhodamine B is an organic dye which dissolves easily in water and widely used in the manufacturing of textile, printing, paper, pharmaceutical and food products [9] [10]. It is allergic to the respiratory system, skin and eyes. It is also a very well-recognized water tracer fluorescent. Rhodamine B is also an important representative of xanthene dyes, and it is usually used as a dye laser material because of its good stability. In recent years, there are many research works focusing on the degradation mechanism of RhB [11] [12] [13], most of them are concerned the mechanism under visible illumination, and N-de-ethylation of RhB is the main degradation mechanism. Therefore, the control against dye wastewater pollution is an important issue to tackle throughout the world.

Copper sulfide is regarded as one of the major p-type semiconductors due to its versatility, availability and low-toxicity nature. In addition, it has excellent optical, electronic and other physical and chemical properties [14]. Due to its good photosensitivity, excellent physical and chemical stability, CuS is an important semiconducting nanomaterial having direct band gap with various potential applications. These applications include catalysis, solar cell, photothermal conversion, gas sensing, lithium ion batteries and nanometer-scale switches [15]. Recently, CuS photocatalytic activity has drawn enormous attention due to their potential applications in the degradation of dye as major ecological contaminants [16]. Mechanistically, CuS photocatalyst is first excited by solar light, which then initiates the photodegradation of pollutants. In the beginning, CuS photocatalyst is excited by light of suitable frequency to generate electrons (e^-). Electrons are then captured by oxygen O_2 to form the superoxide radical anions $O_2^{\bullet-}$ (Equation (2)) and H_2O_2 (Equation (3)) in an oxygen-equilibrated medium. The newly formed intermediates react to form hydroxyl radicals $^\bullet OH$ (Equation (4)). $^\bullet OH$ radical is known to be a very strong oxidant which can easily degrade most pollutants (Equation (5)) [17] [18]:

$$CuS + hv \rightarrow CuS\left(h^+\right) + e^-. \tag{1}$$

$$e^- + O_2 \rightarrow O_2^-. \tag{2}$$

$$e^- + O_2 + 2H_+ \rightarrow H_2O_2. \tag{3}$$

$$H_2O_2 + O_2^{\bullet-} \rightarrow \cdot OH + OH^- + O_2. \tag{4}$$

$$\cdot OH + dey \rightarrow degradation\ products. \tag{5}$$

Natural polysaccharides play an important role in the biosynthesis process of nano-sized semiconductor sulfides [18]. The application of natural organic substances in the preparation of nano-sized material introduces a cutting edge for the charge transfer resulting in major enhancement of photocatalytic efficiency [18] [19]. Aboutaleb, *et al.* [20] prepared PAMAM dendrimer/CuS/AA nanocomposites using gamma irradiation cross-linking method with the aid of sonication. They used the prepared materials to evaluate the removal of Isma acid fast yellow G Dye. The adsorption rate of the dye was found to be almost 85% after 120 min. Wei Shu, *et al.* [21] reported a controlled synthesis of CuS caved super structures and their application to the catalysis of organic dye degradation in the absence of light. They showed that CuS prepared by this method had efficient catalytic activity, making it a cost-effective and convenient method for the treatment of dye-contaminated wastewater. Yu, *et al.* [22] reported that carboxylic acid functionalized graphene oxide-copper (II) sulfide nanoparticle composite (GO-COOH-CuS) was prepared from carboxylated graphene oxide and copper precursor in dimethyl sulfoxide (DMSO) by a facile synthesis process at room temperature. They reported their application to the photocatalytic degradation of phenol and Rhodamine B (RhB), as well as the inactivation of *Escherichia coli* (*E. coli*) and *Bacillus subtilis* (*B. subtilis*) under solar light irradiation using the as-synthesized materials as the photocatalysts. Ghosh, *et al.* [23] also reported a simple electrochemical route to deposit Cu7S4 thin films and their photocatalytic properties. Zang, *et al.* [24] reported biomolecule assisted environmentally friendly one pot synthesis of CuS/RGO nanocomposites with enhanced photocatalytic performance for degradation of Rhodamine B. The main objective of this research project is to focus on newly prepared Gelatin/CuS/PVA nanocomposites initiating the polymerization reaction by γ-ray irradiation. In this work, our aim is to examine the activity of the photocatalytic process of the prepared nanocomposite while monitored against the degradation of Rhodamine B dye under solar irradiation.

2. Experimental

2.1. Materials

Gelatin (Sigma-Aldrich Company) and polyvinyl alcohol (PVA) were used as received. Copper acetate Cu(CH$_3$COO)$_2$·2H$_2$O, Na$_2$S, were purchased from Sigma.

The dye used in these experiments were Rhodamine B (RhB) (λ_{max} = 554 nm). The molecular structure of this organic dye is shown in Figure 1. RhB dye was used without any further purification. Phosphate buffers and other chemicals were all reagent and used as received from their providers.
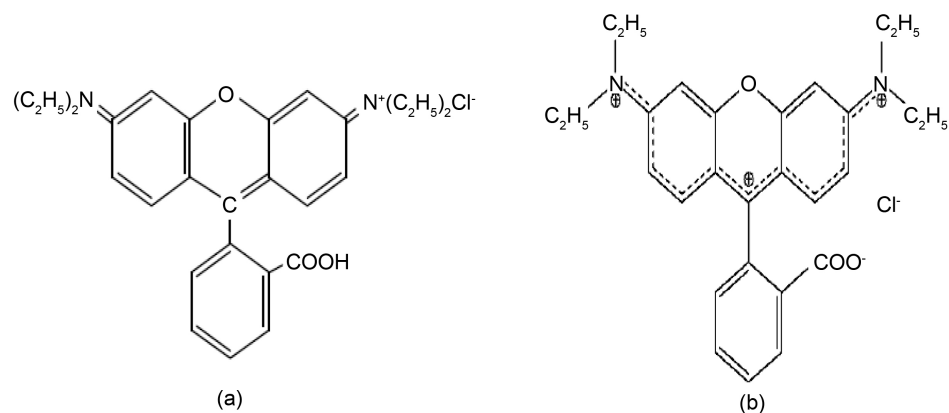
Figure 1. Structure of (a) Rhodamine B (RhB) and (b) Zwitterion Structure of Rhodamine B.

2.2. Synthesis of Gelatin/CuS/PVA Nanocomposites

In a typical method, gelatin/CuS/PVA nanocomposites were prepared according to the method reported in previous work by Abou Taleb, *et al*. [20]. In Particular, 0.3 g of gelatin was dissolved in 30 ml of distilled water under ultrasonic stirring for 1 h at room temperature to form an aqueous solution of 1% concentration. A 5-ml portion of $Cu(CH_3COO)_2 \cdot 2H_2O$ stock aqueous solution (0.2 M) was mixed with 10 ml of the previously prepared gelatin solution and vigorously stirred for 10 min. Consequently, a suitable amount of freshly prepared aqueous solution of Na_2S (0.2 M) was prepared. Subsequently, 10 ml of PVA (10 wt%) was added to the mixed suspension solution and the mixture was stirred for 60 min at 37°C using ultrasonic stirring in order to have a well dispersed solution.

To remove oxygen from the reaction mixture, the mixture was purged with nitrogen for 10 min and then irradiated in Co^{60} γ-ray cell 220 (nordion INT-INC, Intario, Canada) facility of King Abdulaziz City for Science and Technology (KACST), Riyadh, Kingdom of Saudi Arabia. Polymerization reaction was done at 30 kGy at a dose rate of 1.4 kGy/h. After irradiation, the sample was immersed in a solution of glutaraldehyde (0.5% v/v) for 6 h. After the reaction is complete, the produced nanocomposite was washed with absolute alcohol (ethanol) and consequently by doubly distilled water for three times. The sample is finally dried out in an oven at 50°C in air atmosphere.

2.3. Characterization

FT-IR spectra were collected using JASCO-4100 spectrometer. X-ray diffraction (XRD) data were collected using Rigaku 2550D/max VB/PC X-ray diffractometer using Cu Kα radiation (λ = 1.54056Å). SEM; Japan, with an energy dispersive spectroscope (EDS) X-ray spectrometer was used to collect SEM images. TEM images were collected using 2100; JEOL transmission electron microscope.

2.4. RhB Adsorption Isotherms

In a batch adsorption experiment, typically, 10 mg of the photocatalyst and 25 ml of RhB solution with known initial concentration (C_0) is first prepared. The change of RhB concentration is monitored using spectrophotometer (APEL (PD-303 UV)) at 554 nm and the adsorption capacities is calculated using the equation $Qe = V \times (C_0 - C_e)/m$,

where m is the calculated weight of the photocatalyst in grams, C_e is the equilibrium concentration (mg/l), and V is the volume of the solution in liters. Repetition tests were done three times with duplicates each time. Each static adsorption test lasted for 2 h under shaking.

2.5. Photocatalytic Degradation Studies

In a typical photocatalytic experiment, 20 mg of the photocatalyst is suspended in 50 ml of RhB solution (50 mg·l^{-1}) and stirred in the dark for 60 min to insure reaching the adsorption/desorption state of equilibrium. After equilibrium is reached, the nonadsorbed concentration of RhB is measured and taken to be the initial concentration for the photocatalytic process. The reaction mixture is then irradiated under solar light.

Periodically, a 5-ml sample is withdrawn out of the reaction mixture and the extent of degradation is measured using a spectrophotometer at 554 nm. The readings were repeated while the concentration of phenol is varied within the range 25 - 100 ppm. The photodegradation rate for each experiment is calculated using Equation (6):

$$\text{photo degradation rate} = \left(C_0 - C/C_0\right) \times 100. \tag{6}$$

where, C_0 denotes the initial concentration of RhB before illumination and C represents the concentration of RhB in suspension after time t (mg·l^{-1}).

The kinetics of photocatalytic reactions expressed using the concentrations of the photocatalysts can be expressed using the Langmuir-Hinshelwood (L-H) model [25] [26]. When the initial concentration of the reactant (the dye here) is low, Equation (7) holds for the reaction [27].

$$\ln\left(\frac{C_0}{C}\right) = k_{\text{obs}}t. \tag{7}$$

where t the time of irradiation (min) and C_0 is the initial concentration of the photocatalyst (mg/l). The observed rate constant, k_{obs}, can be taken as the apparent first order rate constant of the degradation reaction. A plot of $\ln\left(C_0/C_i\right)$ versus t yields a straight line with a slope of k_{obs}.

The overall uncertainty for all experiments was only 3% - 5%.

3. Results and Discussion

3.1. Catalyst Characterization

3.1.1. FT-IR

FTIR spectrum of gelatin/CuS /PVA (Figure 2(b)) shows many futures that reveals certain changes from that of gelatin/PVA (Figure 2(a)). The broad band at 3365 cm^{-1}, which corresponds to the stretching vibrational modes of -OH, -NH$_2$ and -CONH groups, was shifted to 3321 cm^{-1} and became stronger and broader. This suggests a strong interaction between CuS and these groups. The peak at 623 cm^{-1} corresponds to the characteristic peak of CuS [26]. Also, the spectrum of gelatin/CuS/PVA showed the buildup of the peak at 1654 cm^{-1} and the disappearance of the band at 1596 cm^{-1}, which might be related to the continuous decrease of -NH$_2$ groups as a result of the crosslinking process and the complexation [18]. The FTIR spectrum of gelatin/PVA showed a band around 3400 cm^{-1} indicating the presence of O-H group with polymeric association
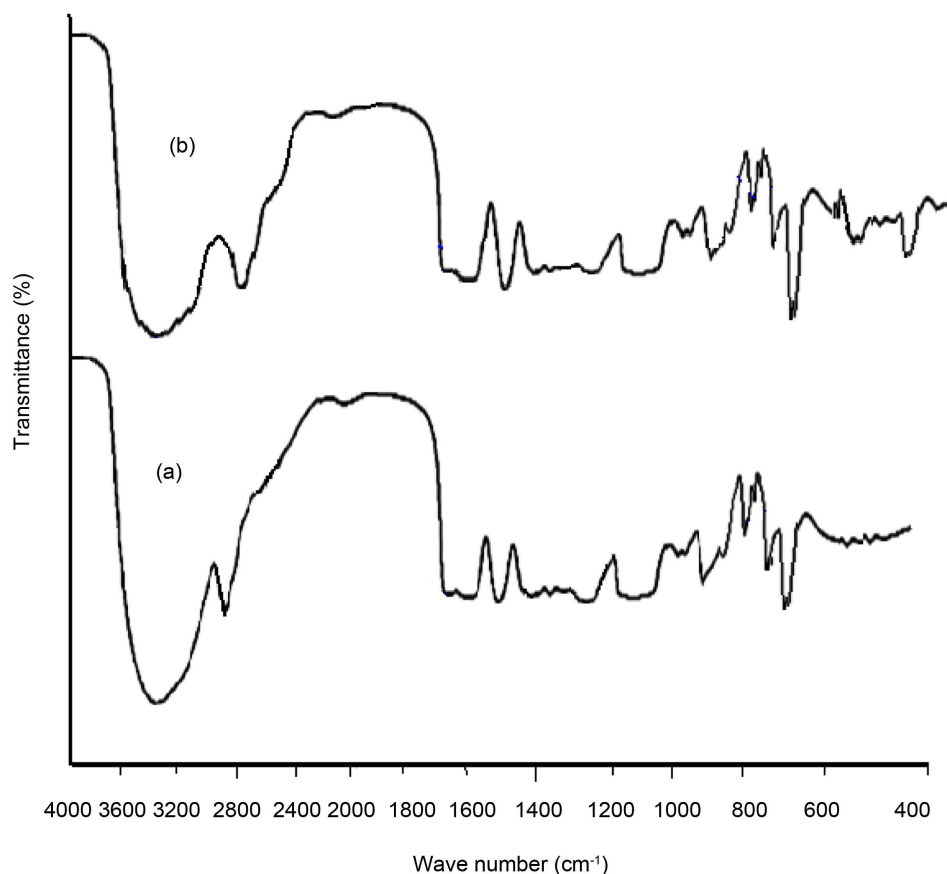
Figure 2. FTIR spectra of (a) gelatin /PVA and (b) gelatin/CuS/PVA.

and a secondary amide. The peak at 1725 cm^{-1} indicates the esterification of PVA and gelatin. All these results align well with previous results reported by Dharmendra, *et al.* [27].

3.1.2. TEM

Figure 3 displays the TEM image of the gelatin/CuS/PVA nanocomposite showing many dark points, referring to homogeneous dispersed nanosized particles with diameters in the range of 20 - 24 nm distributed throughout the matrix. The image indicates that each particle has its own different composition and structure based on the different contrast on every particle. CuS particles are presented by the dark points on the image. The nanoparticals of CuS in the nanocomposites are not equally uniform throughout the matrix [28] [29].

3.1.3. XRD

The XRD data revealed the structures of gelatin/CuS/PVA and gelatin/PVA. The XRD patterns of gelatin/PVA displayed in **Figure 4(a)** showed that the characteristic peak at $2\theta = 20.43$, which coincided with the pattern of the tendon hydrate polymorph of gelatin/PVA reported previously [30]. The XRD patterns for gelatin/CuS/PVA shown in **Figure 4(b)** exhibited the additional peaks at $2\theta = 22.71°$ (004), 32.647° (103) and 36.432° (104) of the crystalline hexagonal CuS (ICSD # 041975 card No. 782391), respectively [31], which indicated that the cubic CuS nanocrystal structure was formed
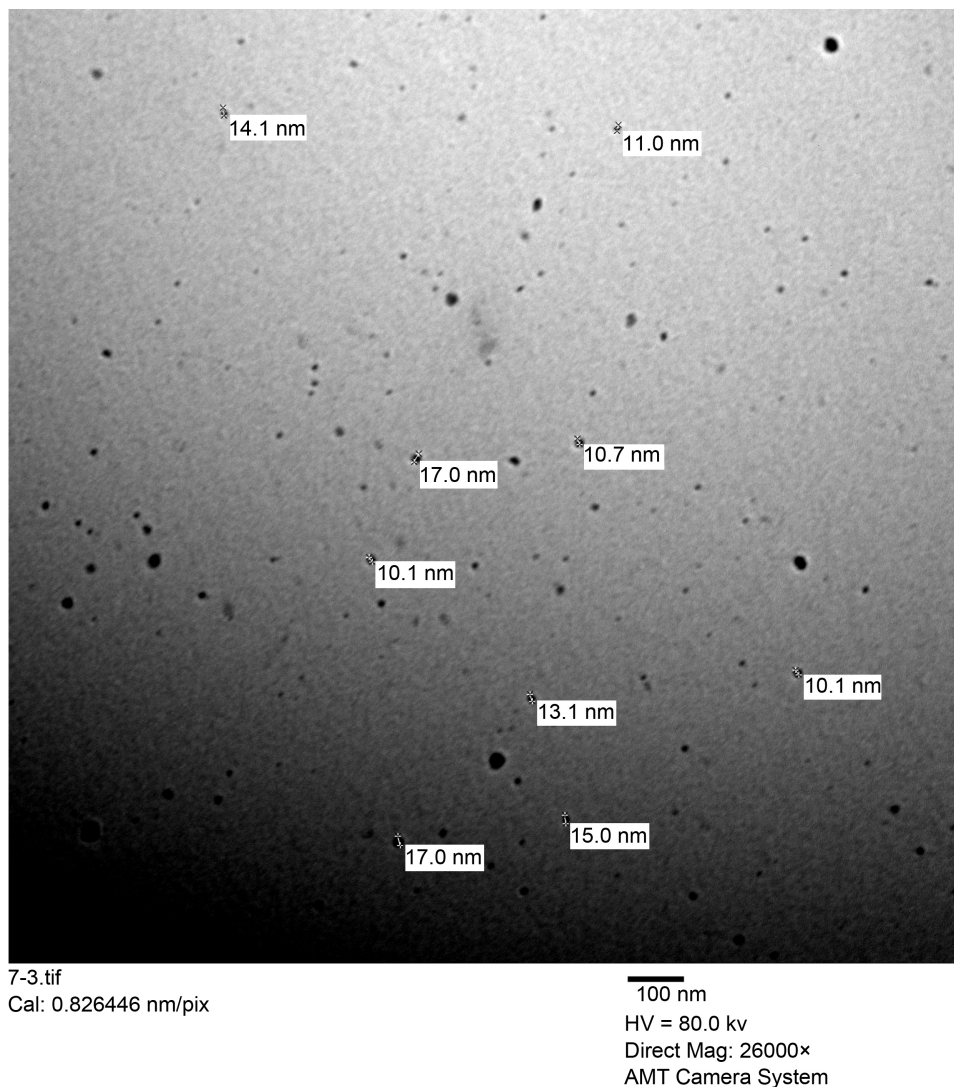
7-3.tif
Cal: 0.826446 nm/pix

100 nm
HV = 80.0 kv
Direct Mag: 26000×
AMT Camera System

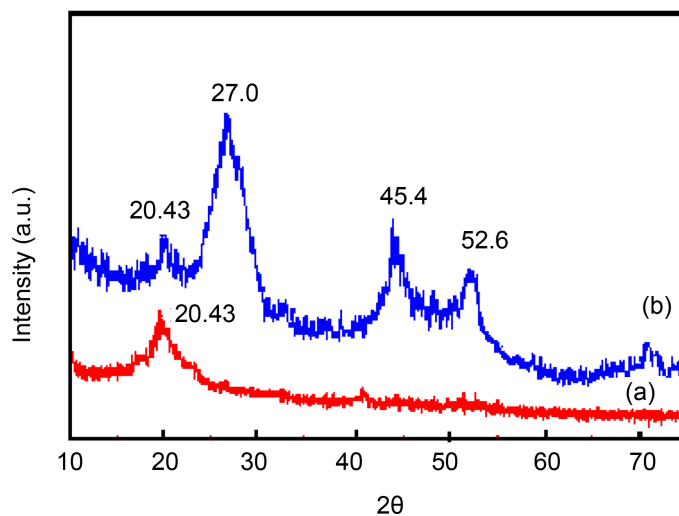**Figure 3.** TEM micrograph of gelatin/CdS/PVA nanocomposite.

Figure 4. XRD patterns of (a) gelatin/PVA and (b) gelatin CdS/PVA nanocomposite.

successfully in the gelatin/CuS/PVA nanocomposite matrix.

Figure 5 displays the EDS spectrum of the synthesized nanocmposite. The appearance of Cu and S peaks confirmed the successful formation of CuS nanostructures.

3.2. Photocatalytic Degradation of RhB

Photocatalytic degradation of RhB was done in a batch reactor and the reaction variables were optimized to maximize the efficiency of degradation process. The essential parameters of the reaction, including: 1) initial RhB concentration, 2) medium pH, and 3) catalyst loading, were varied, and the results are discussed in the next sections.

3.2.1. Photocatalytic Activity

The efficiency of the photocatalysis process of gelatin/CuS/PVA samples were estimated by photocatalytic degradation of RhB aqueous solutions at three different conditions of experiment, and illustrated in Figure 6. It can be seen that almost no RhB
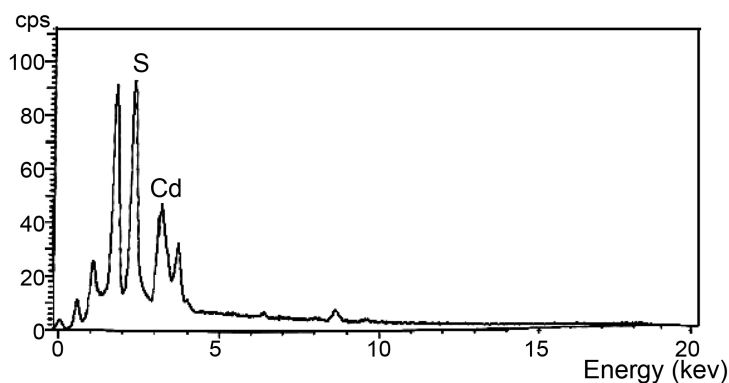
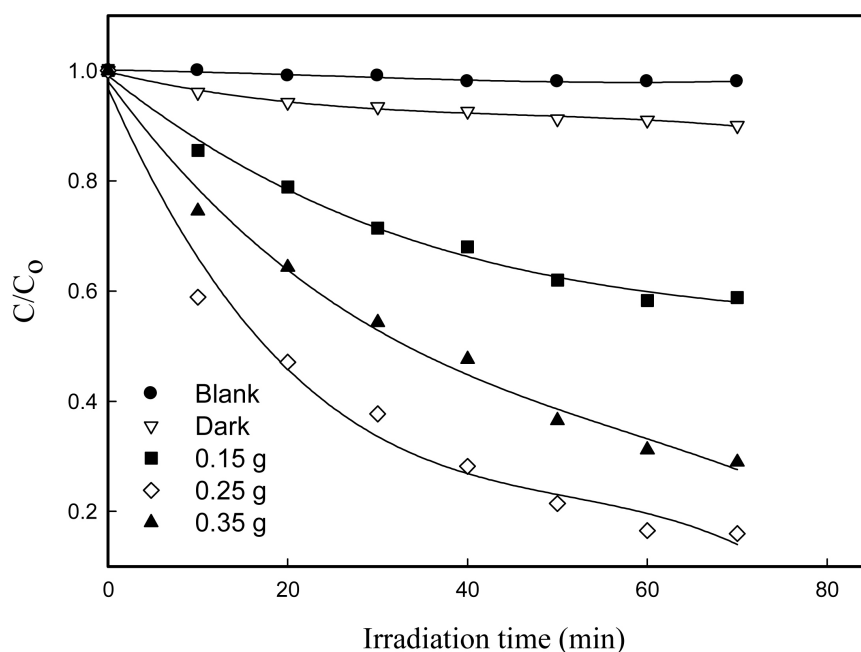**Figure 5.** EDX spectra of gelatin/CdS/PVA nanocomposite.

Figure 6. (a) Visible light induced photocatalytic degradation of RhB over various photocatalysts; (b) kinetics of RhB degradation in solution.

photodegradation for two circumstances: 1) for the mixture of RhB and water in as-mixed state and 2) when the mixture is irradiated while there is no gelatin/CuS/PVA available for Four hours. These results reveal the absence of RhB degradation in such mixtures. There was a slight loss, 8%, in non-irradiated suspensions due to the adsorption of RhB particles on the gelatin/CuS/PVA nanocomposite [10]. Also, it can be noted that the experiment in the absence of photocatalysts showed almost no RhB photodegradation, implying that the self photolysis of RhB is negligible when irradiated with visible light. However, in the presence of gelatin/CuS/PVA nanocomposite, a vast degradation of RhB took place in the presence of irradiation. Such a result apparently indicates that the photocatalytic activity of RhB pollutant degradation is effectively enhanced in the presence of CuS.

3.2.2. Effect of Catalyst Concentration

Photocatalyst concentration is one of the major parameters affecting the efficiency of degradation. To evaluate the photocatalytic activity of the concentration of the photocatayst, a number of experiments were done where the catalyst amount was varied from 0.1 to 0.35 g, at a fixed dye concentration of 25 mg/l. The results of these experiments are displayed in Figure 7(a). The degradation efficient of RhB basic violet dye was observed to increase as the amount of the catalyst dosage increases to 0.25 g. Increasing the concentrations of photocatalyst were thought to increase the absorbance of incident light and produce more generated charge carriers, up to a dosage optimum value at which the maximum photocatalytic activity was observed. But beyond 0.25 g, there is a decrease in photocatalytic activity of RhB [32]. This can be attributed to the fact that the solution becomes turbid and hence cause shielding of light and hinder the light penetration. In addition, it might not be possible to continuously inject the photons into photocatalyst particles and a combination of electrons and holes may have been accelerated there [33].
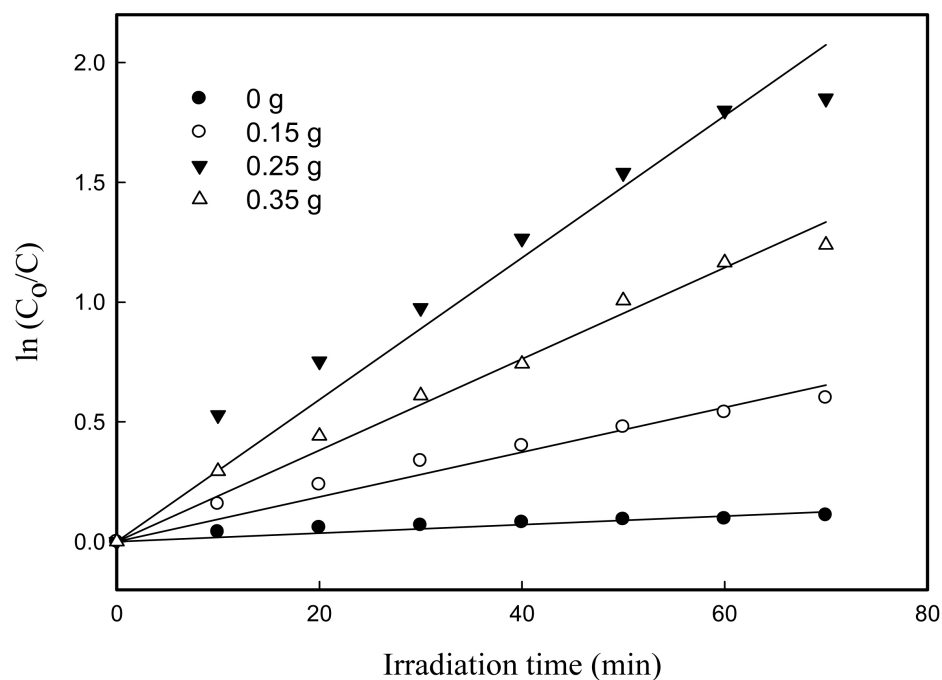
The photocatalytic degradation n of RhB is a pseudo first-order eaction and its kinetics is found to fit the expression given Equation (7): The linear graph of $-\ln C_0/C$ versus t (min) confirms the pseudo first-order reaction for RhB degradation. The apparent rate constant k_{obs} (min^{-1}) increases with increasing the amount of catalyst dosage upto 0.25 g when other parameters are kept constant as shown in Figure 7(b). The observed reaction rate constants (k_{obs}) of the catalysts, which have pseudo first order kinetics, and the coefficients of the linear regression, are tabulated in Table 1. The results listed in the table confirm the interpenetrations mentioned earlier where the increase in the catalyst concentration leads to an increase in the reaction rate. The observed increase in rate constants as a result of increasing the amount of the catalyst could be attributed to the increase in the number of photons absorbed and the number of dye molecule adsorbed [34]. Table 1 shows also that the photocatalytic activity of the polymeric nanocomposites is high as can be seen from the large value of k_{obs}.

3.2.3. Effect of the Initial Concentration of RhB Dye

The effect of the initial concentration of the dye on the efficiency of the photocatalytic degradation was investigated, as it represents an essential parameter in the degradation reactions of organic contaminants. Concentrations of RhB in the range of 25 - 100 mg/l
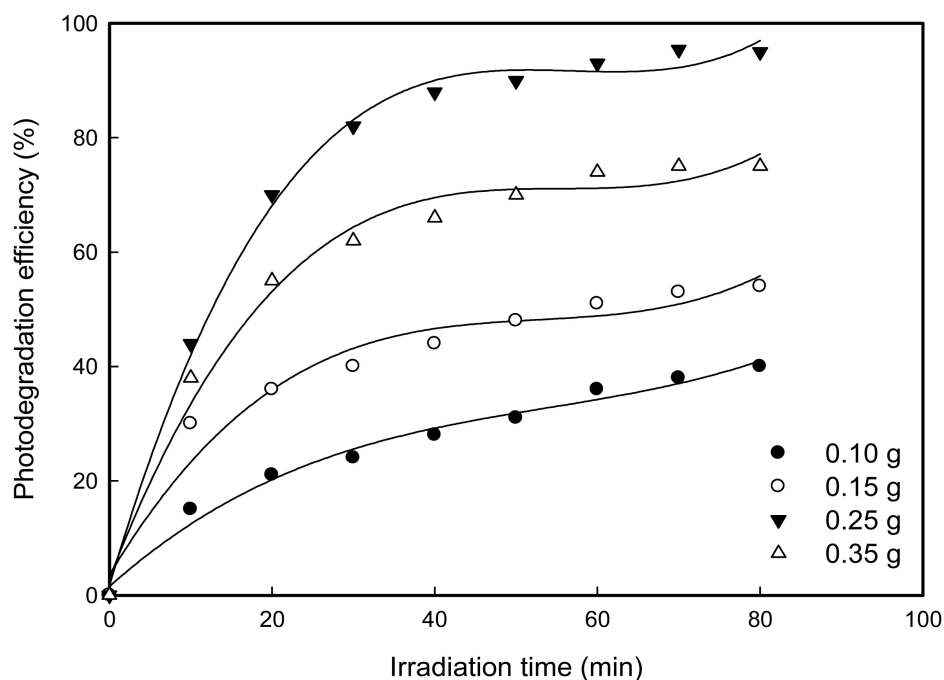
(a)

(b)

Figure 7. (a) Effect of irradiation time (min) on photocatalytic degradation of RhB onto gelatin/CdS/PVA nanocomposite. Control: temp.: 30°C; t: 80 min at different of catalyst amount (b) first-order photo-degradation kinetics at different of catalyst amount.

were investigated, and the results are shown in **Figure 8(a)**. The efficiency of photocatalytic degradation of RhB tended to decrease with increasing the concentration of RhB. Similar trends have been observed for the photocatalytic oxidation of other organic
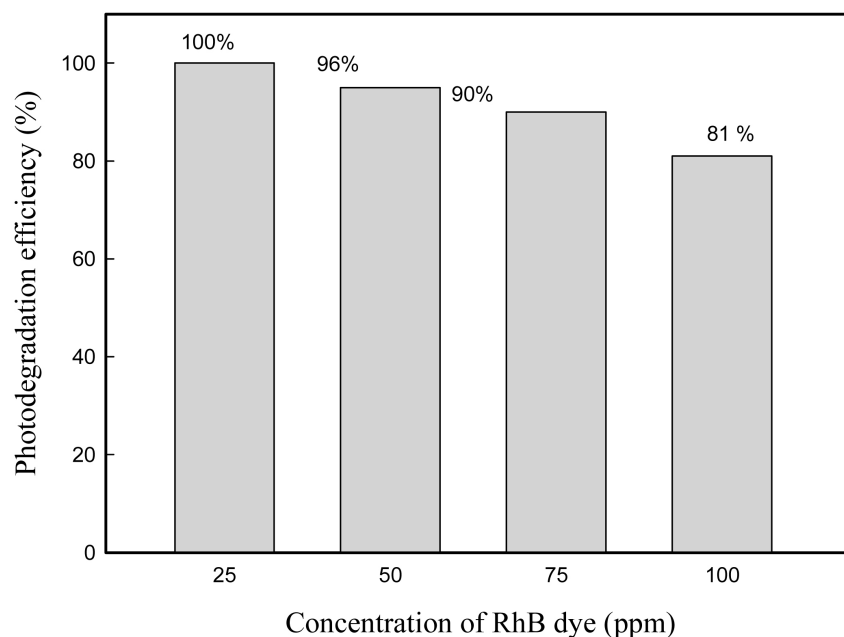
Figure 8. Effect of initial RhB concentration on the photodegradation efficiency (catalyst amount = 0.1 g/100 ml).

Table 1. Pseudo-first order rate constants for the degradation and linear regression coefficients of the catalyst amount of gelatin/CdS/PVA as photocatalyst.

Catalyst	k_{obs} (min^{-1})	R^2
0.0 g	1.383×10^{-3}	0.94
0.10 g	8.218×10^{-3}	0.978
0.25 g	2.614×10^{-2}	0.975
0.35 g	1.769×10^{-2}	0.987

compounds [7] [10] [33]. A possible explanation for this behavior is that the production of $^\bullet$OH radical on the surface of the catalyst is reduced as the initial concentration of RhB is increased. As the number of RhB molecules adsorbed on the surface of gelatin/CuS/PVA photocatalystis increases, the number of active sites available for the $^\bullet$OH adsorption dramatically decreases. The transmittance of the solution decreases with increasing the concentration, leading to fewer photons reaching the photocatalyst surface capable of activating it to generate $^\bullet$OH and $O_2^{\bullet-}$ radicals. Therefore, large number of adsorbed RhB molecules would inhibit the reaction between RhB molecules and $^\bullet$OH radicals as a result of the less chance of any direct interaction between them.

3.2.4. Influence of Initial pH on Gelatin/CuS/PVA Photocatalyst

Changing the medium pH affects the number of available adsorption sites on the catalyst. Changing the medium pH can also alter the charge of the pollutants and the catalyst, and consequently the adsorption rate on the active sites of the catalyst [35].

Figure 8(b) shows the effect of changing the pH of the solution on the efficiency of the photodegradation process. Experiments were carried out at various pH values, ranging from 2 to 11 at a fixed concentration of the dye of (25 ppm). It can be easily

seen that the efficiency of the degradation of RhB increases as the value of pH increases up to a pH of 10. After this value, efficiency decreases as pH increases.
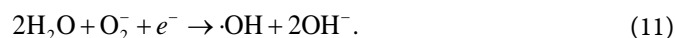
The variation is not because of the little change in the absorption of radiation as λ_{mx} for the RhB dye changes very little (from 551 to 553 nm) when the pH changes from 2 to12 even though RhB exists in two principal forms in water, *i.e.* cationic (RhB$^+$) and zwitter ionic (RhB$^\pm$) [36] [37]. In the acidic range, the dye presents in cationic form (RhB$^+$). Therefore, electrostatic repulsion may occur between RhB and the catalysts, resulting in the decrease of the degradation efficiency. At higher pH value, the RhB$^+$ gets deprotonated and its zwitter ion is formed (**Figure 1**). In addition, basic pH conditions might help in the production of ·OH radicals, which makes the degradation through ·OH radical oxidation mechanism possible. All of these can promote the degradation of RhB and the reaction intermediates. Above a pH of 10, the concentration of OH$^-$ ions would be high enough to cover the surface of the catalyst and hence cause it to be negatively charged. Because RhB dye is not protonated at a pH higher than 10, it will be repelled by the negatively charged surface of catalysis. Therefore, the efficiency of the degradation process decreases as the medium pH exceeds the value of 10.

3.2.5. Photocatalytic Reaction Mechanism

Composite materials have been successfully used to reduce the hole-electron pair recombination accompanying photocatalytic processes. Wide range of materials, including metals, metal oxides and organic molecules are used for the preparation of such composite materials [11] [38]. Semiconductor nanocomposites, when irradiated, are found to be capable of eliminating different organic pollutants in the presence of oxygen. A semiconductor is activated on the surface of the catalyst by a photon of light ($h\upsilon$) to produce electron-hole pairs which are strong oxidizing and reducing agents:

$$\text{Semiconductor nanocomposite} + h\upsilon \rightarrow h^+ + e^-. \tag{8}$$
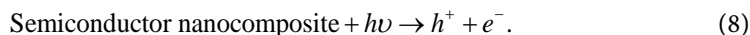
Most of electrons and holes that are photo-generated react with water and molecular oxygen according to the reactions [39]:

$$\text{H}_2\text{O} + h^+ \rightarrow \cdot\text{OH} + \text{H}^+. \tag{9}$$

$$\text{O}_2 + e^- \rightarrow \text{O}_2^-. \tag{10}$$

$$2\text{H}_2\text{O} + \text{O}_2^- + e^- \rightarrow \cdot\text{OH} + 2\text{OH}^-. \tag{11}$$

$$\text{OH}^- + h^+ \rightarrow \cdot\text{OH}. \tag{12}$$

In fact, ·OH radical is a strong oxidant that can very easily degrade most contaminants. Presence of O$_2$ may inhibit the re-combination of hole-electron pairs. Successive reactions lead to the oxidation of RhB dye and the complete photodegradation. Normally, RhB is very stable under light irradiation when no catalyst is available. A possible mechanism for the degradation of RhB is suggested to involve three steps: 1) N-deethylation, 2) cleavage of chromophore and 3) mineralization of the dye (**Figure 9**) [7], [11] [40].

4. Conclusion

This research project led to results supporting the fact that the gelatin/CuS/PVA nano-
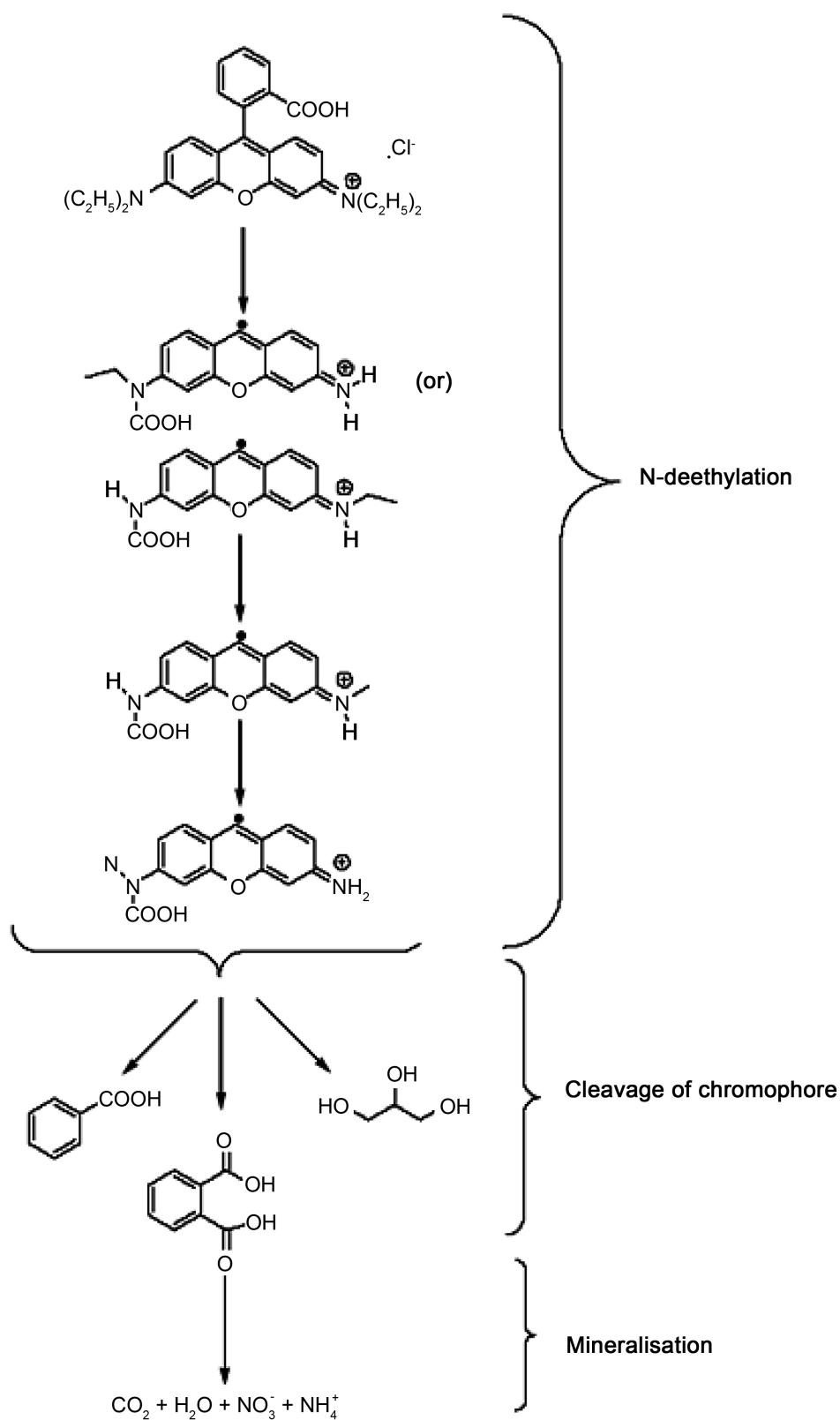
Figure 9. Possible photocatalytic decoloration pathway for the photocatalytic degradation of RhB dye under solar light irradiation [7].

composite can efficiently catalyze the photodegradation of RhB dye under solar light.

Gelatin/CuS/PVA nanocomposites were successfully synthesized using gamma radiation induced copolymerization. The preparation of gelatin/CuS/PVA nanocomposite was confirmed qualitatively by FTIR and XRD. The particle size distribution obtained from the TEM results was found to range from 20 to 24 nm, which clearly referred to CuS nanocomposites. These particles are randomly distributed and are not equally uniformed. The rate of photocatalytic degradation reaction of the mono-substituted RhB dye was found to be sensitive to the pH of the reaction medium. This sensitivity might be attributed to the effect of the pH values on the surface characteristics of gelatin/CuS/PVA nanocomposite and to the distribution of reaction species as well. RhB dye photocatalytic degradation under solar light worked best at low initial concentration of RhB dye. The efficiency of photocatalytic degradation was found to decrease as the initial concentration of phenol was increased. High efficiency of photocatalytic degradation was also observed at a pH of 10 of the reaction medium. RhB photocatalytic degradation in aqueous gelatin/CuS/PVA nanocomposite was found to follow a pseudo-first-order kinetics. The results of these studies clearly reveal the importance of identifying the optimum parameters for the degradation process in order to enhance the rate of degradation. This is necessary for any real and effective application of photocatalytic oxidation processes. Moreover, the outcomes of these investigations showed how gelatin/CuS/PVA nanocomposites can work as effective and convenient photocatalysts for removing RhB dye from wastewater through degradation process.

References

[1] Papić, S., Koprivanac, N., Božić, A. and Meteš, M. (2004) Removal of Some Reactive Dyes from Synthetic Wastewater by Combined Al(III) Coagulation/Carbon Adsorption Process *Dyes and Pigments*, **62**, 291-298. https://doi.org/10.1016/S0143-7208(03)00148-7

[2] Shannon, M.A., Bohn, P.W., Elimelech, M., Georgiadis, J.G., Mariñas, B.J. and Mayes, A.M. (2008) Science and Technology for Water Purification in the Coming Decades. *Nature*, **452**, 301-310. https://doi.org/10.1038/nature06599

[3] Qourzal, S., Barka, N., Tamimi, M., *et al.* (2008) Photodegradation of 2-Naphthol in Water by Artificial Light Illumination Using TiO_2 Photocatalyst: Identification of Intermediates and the Reaction Pathway. *Applied Catalysis A*: *General*, **334**, 386-393. https://doi.org/10.1016/j.apcata.2007.09.034

[4] Hu, Y. and Yuan, C. (2005) Low-Temperature Preparation of Photocatalytic TiO_2 Thin Films from Anatase Sols. *Journal of Crystal Growth*, **274**, 563-568. https://doi.org/10.1016/j.jcrysgro.2004.10.146

[5] Taleb, M.F.A. (2014) Adsorption and Photocatalytic Degradation of 2-CP in Wastewater onto $CS/CoFe_2O_4$ Nanocomposite Synthesized Using Gamma Radiation. *Carbohydrate Polymers*, **114**, 65-72. https://doi.org/10.1016/j.carbpol.2014.07.061

[6] Hong, Y., Ren, A., Jiang, Y., *et al.* (2015) Sol-Gel Synthesis of Visible-Light-Driven $Ni_{(1-x)}Cu_{(x)}Fe_2O_4$ Photocatalysts for Degradation of Tetracycline. *Ceramics International*, **41**, 1477-1486. https://doi.org/10.1016/j.ceramint.2014.09.082

[7] Liu, S.W., Yu, J.G. and Jaroniec, M. (2010) Tunable Photocatalytic Selectivity of Hollow TiO_2 Microspheres Composed of Anatase Polyhedra with Exposed {001} Facets. *Journal of the American Chemical Society*, **132**, 11914-11916. https://doi.org/10.1021/ja105283s

[8] Xie, Y., Zhang, S., Pan, B., *et al.* (2011) Effect of CdS Distribution on the Photocatalytic Performance of Resin-CdS Nanocomposites. *Chemical Engineering Journal*, **174**, 351-356.

https://doi.org/10.1016/j.cej.2011.09.006

[9] Mittal, A., Malviya, A., Kaur, D., *et al.* (2007) Studies on the Adsorption Kinetics and Isotherms for the Removal and Recovery of Methyl Orange from Wastewaters Using Waste Materials. *Journal of Hazardous Materials*, **148**, 229-240. https://doi.org/10.1016/j.jhazmat.2007.02.028

[10] Richardson, S.D., Willson, C.S. and Rusch, K.A. (2004) Use of Rhodamine Water Tracer in the Marshland Upwelling System. *Ground Water*, **42**, 678-688. https://doi.org/10.1111/j.1745-6584.2004.tb02722.x

[11] Cotto-Maldonado, M. (2013) Photocatalytic Degradation of Rhodamine-B under UV-Visible Light Irradiation Using Different Nanostructured Catalysts. *American Chemical Science Journal*, **3**, 178-202. https://doi.org/10.9734/ACSJ/2013/2712

[12] Sun, M., Li, D., Chen, Y., Chen, W., Li, W., *et al.* (2009) Synthesis and Photocatalytic Activity of Calcium Antimony Oxide Hydroxide for the Degradation of Dyes in Water. *Journal of Physical Chemistry C*, **113**, 13825-13831. https://doi.org/10.1021/jp903355a

[13] Rajalakshmi, S., Pitchaimuthu, S., Kannan, N. and Velusamy, P. (2014) Enhanced Photocatalytic Activity of Metal Oxides/β-Cyclodextrin Nanocomposites for Decoloration of Rhodamine B Dye under Solar Light Irradiation. *Applied Water Science*, 1-13.

[14] Dhasade, S.S., Patil, J.S., Thombare, J.V. and Fulari, V.J. (2015) Studies on Synthesis and Characterization of Copper Sulfide Thin Films. *Science & Technology*, **41**, 1-3.

[15] Feng, C., Zhang, L., Yang, M., Song, X., Zhao, H., Jia, Z., Sun, K. and Gao, L. (2015) One-Pot Synthesis of Copper Sulfide Nanowires/Reduced Graphene Oxide Nanocomposites with Excellent Lithium-Storage Properties as Anode Materials for Lithium-Ion Batteries. *ACS Applied Materials & Interfaces*, **7**, 15726-15734. https://doi.org/10.1021/acsami.5b01285

[16] Sreelekha, N., Subramanyam, K., Amaranatha, R.D., *et al.* (2016) Structural, Optical, Magnetic and Photocatalytic Properties of Co Doped CuS Diluted Magnetic Semiconductor Nanoparticles. *Applied Surface Science*, **378**, 330-340. https://doi.org/10.1016/j.apsusc.2016.04.003

[17] Lu, Y.Y., Zhang, Y.Y., Zhang, J., *et al.* (2016) *In Situ* Loading of CuS Nanoflowers on Rutile TiO$_2$ Surface and Their Improved Photocatalytic Performance. *Applied Surface Science*, **370**, 312-319. https://doi.org/10.1016/j.apsusc.2016.02.170

[18] Saranya, M., Ramachandran, R., Samuel, E.J.J., Jeongc, S. and Grace, A. (2015) Enhanced Visible Light Photocatalytic Reduction of Organic Pollutant and Electrochemical Properties of CuS Catalyst. *Powder Technology*, **279**, 209-220. https://doi.org/10.1016/j.powtec.2015.03.041

[19] Chan, W.C.W., Maxwell, D.J., Gao, X., Bailey, R.E., Han, M. and Nie, S. (2002) Luminescent Quantum Dots for Multiplexed Biological Detection and Imaging. *Current Opinion in Biotechnology*, **13**, 40-46. https://doi.org/10.1016/S0958-1669(02)00282-3

[20] Abou Taleb, M.F., El-Trass, A. and El-Sigeny, S. (2015) Synthesis of Polyamidoamine Dendrimer (PAMAM/CuS/AA) Nanocomposite and Its Application in the Removal of Isma Acid Fast Yellow G Dye. *Polymers for Advanced Technologies*, **26**, 994-1002. https://doi.org/10.1002/pat.3517

[21] Shu, Q., Lan, J., Gao, M., Wang, J. and Huang, C.Z. (2015) Controlled Synthesis of CuS Caved Superstructures and Their Application to the Catalysis of Organic Dye Degradation in the Absence of Light. *CrystEngComm*, **17**, 1374-1380. https://doi.org/10.1039/C4CE02120G

[22] Yu, S., Liu, J., Zhu, W., *et al.* (2015) Facile Room-Temperature Synthesis of Carboxylated Graphene Oxide-Copper Sulfide Nanocomposite with High Photodegradation and Disinfection Activities under Solar Light Irradiation. *Scientific Reports*, **5**, 148-155.

[23] Amrita Ghosh, A.M. (2015) A Simple Electrochemical Route to Deposit Cu_7S_4 Thin Films and Their Photocatalytic Properties. *Applied Surface Science*, **328**, 63-70. https://doi.org/10.1016/j.apsusc.2014.12.032

[24] Zhang, Y., Tian, J., Li, H., Wang, L., Qin, X., Asiri, A.M., Al-Youbi, A.O. and Sun, X. (2012) Biomolecule Assisted Environmentally Friendly, One-Pot Synthesis of CuS/Reduced Graphene Oxide Nanocomposites with Enhanced Photocatalytic Performance. *Langmuir*, **28**, 12893-12900. https://doi.org/10.1021/la303049w

[25] Chen, H.Y., Zahraa, O., Bouchy, M., Thomas, F. and Bottero, J.Y. (1995) Adsorption Properties of TiO_2 Related to the Photocatalytic Degradation of Organic Contaminants in Water. *Journal of Photochemistry and Photobiology A*: *Chemistry*, **85**, 179-186. https://doi.org/10.1016/1010-6030(94)03900-F

[26] Wang, Y., Zhang, L., Jiu, H., Li, N. and Su, Y. (2014) Depositing of CuS Nanocrystals upon the Graphene Scaffold and Their Photocatalytic Activities. *Applied Surface Science*, **303**, 54-60. https://doi.org/10.1016/j.apsusc.2014.02.058

[27] Jain, D., Carvalho, E., Banthia, A.K. and Banerjee, R. (2011) Development of Polyvinyl Alcohol-Gelatin Membranes for Antibiotic Delivery in the Eye. *Drug Development and Industrial Pharmacy*, **37**, 167-177. https://doi.org/10.3109/03639045.2010.502533

[28] Kumar, V., Pathania, D., Agarwal, S. and Singh, P. (2012) Adsorptional Photocatalytic Degradation of Methylene Blue onto Pectin-CuS Nanocomposite under Solar Light. *Journal of Hazardous Materials*, **243**, 179-186. https://doi.org/10.1016/j.jhazmat.2012.10.018

[29] Al-Kahtani, A.A. and Abou Taleb, M.F. (2016) Photocatalytic Degradation of Maxilon C.I. Basic Dye Using $CS/CoFe_2O_4/GONCs$ as a Heterogeneous Photo-Fenton Catalyst Prepared by Gamma Irradiation. *Journal of Hazardous Materials*, **309**, 10-19. https://doi.org/10.1016/j.jhazmat.2016.01.071

[30] Pal, K., Banthia, A.K. and Majumdar, D.K. (2007) Preparation and Characterization of Polyvinyl Alcohol-Gelatin Hydrogel Membranes for Biomedical Applications. *AAPS PharmSciTech*, **8**, E142-E146. https://doi.org/10.1208/pt080121

[31] Shanan, Z.J. (2015) Synthesis and Characterization of CuS/PVA Nanocomposite via Chemical Method. *IOSR Journal of Research & Method in Education*, **5**, 2320-7388.

[32] Cui, W., An, W., Liu, L., Hu, J. and Liang, Y. (2014) Synthesis of CdS/BiOBr Composite and Its Enhanced Photocatalytic Degradation for Rhodamine B. *Applied Surface Science*, **319**, 298-305. https://doi.org/10.1016/j.apsusc.2014.05.179

[33] Bao, N., Shen, L., Takata, T. and Domen, K. (2008) Self-Templated Synthesis of Nanoporous CdS Nanostructures for Highly Efficient Photocatalytic Hydrogen Production under Visible Light. *Chemistry of Materials*, **20**, 110-117. https://doi.org/10.1021/cm7029344

[34] Jiang, R., Zhu, H., Li, X. and Xiao, L. (2009) Visible Light Photocatalytic Decolourization of C. I. Acid Red 66 by Chitosan Capped CdS Composite Nanoparticles. *Chemical Engineering Journal*, **152**, 537-542. https://doi.org/10.1016/j.cej.2009.05.037

[35] Antoniou, M.G. and Dionysiou, D.D. (2007) Application of Immobilized Titanium Dioxide Photocatalysts for the Degradation of Creatinine and Phenol, Model Organic Contaminants Found in NASA's Spacecrafts Wastewater Streams. *Catalysis Today*, **124**, 215-223. https://doi.org/10.1016/j.cattod.2007.03.054

[36] Li, Y. and Chen, W. (2011) Photocatalytic Degradation of Rhodamine B Using Nanocrystalline TiO_2-Zeolite Surface Composite Catalysts: Effects of Photocatalytic Condition on Degradation Efficiency. *Catalysis Science & Technology*, **1**, 802-809. https://doi.org/10.1039/c1cy00012h

[37] Hariprasad, N., Anju, S.G., Yesodharan, E.P. and Suguna, Y. (2013) Sunlight Induced Removal of Rhodamine B from Water through Semiconductor Photocatalysis: Effects of Adsorption, Reaction Conditions and Additives. *Research Journal of Material Sciences*, **1**,

9-17.

[38] Mu, J., Chen, B., Zhang, M., *et al.* (2012) Enhancement of the Visible-Light Photocatalytic Activity of In_2O_3-TiO_2 Nanofiber Heteroarchitectures. *ACS Applied Materials & Interfaces*, **4**, 424-430. https://doi.org/10.1021/am201499r

[39] Soltani, N., Saion, E., Mat, W.M., *et al.* (2014) Applied Surface Science Enhancement of Visible Light Photocatalytic Activity of ZnS and CdS Nanoparticles Based on Organic and Inorganic Coating. *Applied Surface Science*, **290**, 440-447. https://doi.org/10.1016/j.apsusc.2013.11.104

[40] Li, Z., Xie, Z., Zhang, Y., Wu, L., Wang, X. and Fu, X. (2007) Wide Band Gap p-Block Metal Oxyhydroxide InOOH: A New Durable Photocatalyst for Benzene Degradation. *Journal of Physical Chemistry C*, **111**, 18348-18352. https://doi.org/10.1021/jp076107r